Likelihood of detection and computational complexity of GPS acquisition algorithms

Staffan Backén, *Luleå University of Technology*

ABSTRACT

A key parameter of GNSS receiver performance is the sensitivity, meaning how weak signals the receiver can acquire and track. For acquisition, this is typically measured by the minimum signal strength that can be detected with a certain probability.

In this paper, a novel method of computing the probability of detection is presented. In contrast with prevailing techniques, it takes receiver parameters such as correlator and doppler spacing into account when computing the probability distribution function. The likelihood of data bit switches inside the correlation window is also considered in a similar fashion.

The method is demonstrated both on a traditional correlator architecture, and on two different FFT based acquisition algorithms, coherent and non-coherent. Further, the computational complexity of the different algorithms is evaluated for a general computing platform. The combination of these two methods provide valuable insight into the problem of minimizing power consumption while maximizing sensitivity for software based GNSS receivers.

1 INTRODUCTION

GNSS (Global Navigation Satellite Systems) have over the last decade established itself as a fundamental infrastructure. Mass market receivers have utilized both the increased processing power, enabled by technological advancements in micro electronics, and modern digital signal processing techniques to achieve increased performance. A fundamental parameter is the receiver sensitivity, meaning how weak signals a receiver can acquire (detect) and track.

At present, the most utilized signal is the GPS C/A code, a CDMA (Code Division Multiple Access) signal. While significant research efforts have been targeted at optimizing acquisition algorithms for this signal, the general detection problem have been studied for much longer. A fundamental resource is written by (Marcum, 1960), and since then many articles have been written on the subject. In general, a signal plus noise is received. When the power of the signal is low compared to the power of the noise, some method of integration is required to increase the SNR (signal to noise ratio) to allow for a reliable detection. Depending on the nature of the noise and the signal, this method may be fairly complicated. When evaluating the performance of the detector, the PDFs (probability distribution functions) of noise and noise+signal is a central resource. Unfortunately, for more complicated detectors, the PDFs may not exist in closed form. Of particular interest for GNSS acquisition is the non-coherent summation. Lowe treated this in a general context (Lowe, 1999), and Beaulieu proposed closed form approximations (Beaulieu, 1990).

Software based GNSS receivers (Akos, 1997) is now common. One reason for this is a method where the resource intensive correlation function is computed using the FFT algorithm (van Nee and Coenen, 1991). Among other, Psiaki have investigated acquisition algorithms for software based GPS receivers (Psiaki, 2001). Today, with modern processing elements, the desired sensitivity is usually possible to achieve. However, hand held receivers have tightly constrained power budgets. As a consequence, the sensitivity per watt should be the unit of measurement for acquisition algorithms.

This paper attempts to derive a metric that is reasonably close to this, while also proposing novel methods regarding computing the sensitivity. For two common FFT-based acquisition algorithms, the number of operations on a hypothetical computing engine is evaluated. It is believed that this measurement is reasonably proportional to the desired estimate of power consumption. Also, several additional effects are considered when evaluating the probability density functions. Correlator and doppler spacing is integrated into the PDFs, as well as the likelihood of a data bit switch during the integration period.

The paper is outlined as follows. First, the signal model is presented together with several realistic estimates. Second, a straight forward serial search algorithm is shown to exemplify the methods used to arrive at the accurate

S. Backén is with the Department of Electrical Engineering and Computer Science, Luleå University of Technology, Luleå, 97187 Sweden e-mail: staffan@csee.ltu.se. This work was supported in part by the Swedish national graduate school of space technology.

PDFs. This section is followed by a detailed description of a coherent FFT-based acquisition algorithm. A non-coherent version is presented next. Finally, the paper is concluded.

2 SIGNAL MODEL

In this section, the structure of the civilian GPS C/A-code signal will be described. Physical effects, such as clock frequency offsets, will be discussed with the intent of presenting a concise model of the received signal.

The C/A code signal as transmitted from an individual satellites at time t_t can be described as

$$s_t(t_t) = A_t \cos(2\pi f_0 t_t)\, m_{sv}(f_m t_t) \tag{1}$$

where A_t is the amplitude and the function $m_{sv}()$ represent the BPSK modulation, $f_0 = 1575.42\,\text{MHz}$ and $f_m = 1.023\,\text{MHz}$ $\left(\frac{f_c}{f_m} = 1540\right)$. $m_{sv}(n)$ contains both a pseudo-noise sequence and data bits from satellite sv as

$$m_{sv}(n) = PN_{sv}[\lfloor n \rfloor \mod 1023]\, DB_{sv}\left[\left\lfloor \frac{n}{20} \right\rfloor \mod L\right] \tag{2}$$

where PN_{sv} represent a 1023 element long repeating pseudo-noise vector unique for every satellite sv. The "$\lfloor\rfloor$" notation means the floor() function. $PN_{sv} \in [-1,1]$, and it is further designed to minimize cross correlation with the signals transmitted from other satellites. Finally, the function $DB_{sv}()$ describes the data bits transmitted, where $DB_{sv} \in [-1,1]$ is a 12.5 minutes long sequence ($L = 37500$) containing time stamps, orbital parameters et cetera. These change over time and thus new versions of DB_{sv} are periodically uploaded from the GPS control stations. It should be noted that although the satellite time t_t is derived from an onboard high quality atomic clock, it is obviously not perfect. While it does drift slightly over time, the ratio of carrier cycles over code chips (one "bit" of the pseudo noise code) remains at 1540 and as such the carrier, code and data bits remain synchronized. The transmitted signal have a null to null main lobe bandwidth of 2.046 MHz due to the modulation rate.

After $60-80\,\text{ms}$ the transmitted signal will impinge on the antenna of the receiver. After amplification, filtering, mixing and quantization in the front-end, a digital replica of the signal is input to the baseband processor. In this paper, we will assume a front-end with the following properties:

1. Ideal filter with a passband of 2.046 MHz
2. A nominal sampling rate f_{s_0} of 2.048 MHz
3. I/Q (complex) sampling
4. An ADC with infinite resolution
5. A local oscillator with a maximum error of 2 ppm
6. No in-band RF interference and negligible C/A code cross-correlation/auto-correlation

The sampling rate, filter bandwidth and I/Q sampling is chosen for several reasons. First, the main lobe of the signal (2.046 MHz) contains the majority (around 90%) of the signal power. While a larger bandwidth is desirable for tracking (due to better capability of mitigating multi-path (van Dierendonck et al., 1992)), it requires processing more samples while only being marginally beneficial with regards to detection capability. Secondly, rapid acquisition algorithms is based on the FFT in some form, and as such benefit from a data length that is a power of two[1]. The C/A code length is 1 ms, corresponding to $2048 = 2^{11}$ samples. The FFT algorithms also favor complex sampling.

Assumption 4 is not realistic, although given that the loss in SNR for CDMA applications when using a 4-bit ADC is only a fraction of a dB (Bastide et al., 2003), it is a reasonable simplification. The oscillator parameters are typical for a high quality TCXO. Finally, RF interference and C/A code cross-correlation is ignored for the sake of simplicity. The received signal we will consider in this paper is

$$s[n] = A(t_n)\cos(2\pi f_{carr}(t_n)\, t_n + \phi)\, m(f_{code}(t_n)\, t_n + \tau) + \omega(t_n) \tag{3}$$

where n is the sample index, A is the amplitude and t_n is the time corresponding to sample n. The carrier (cosine term) depends on the carrier frequency $f_{carr}(t_n)$, t_n and phase ϕ. The code $m()$ depends on the code frequency $f_{code}(t_n)$, t_n and code phase τ. Finally, the noise ω is assumed to be white and gaussian. The time t_n is related to the sample number n as

$$n = \int_0^{t_n} f_s(t_n) \tag{4}$$

where $f_s(t_n)$ is the sampling frequency at time t_n.

The carrier frequency f_{carr} is nominally 0, although it depends on satellite range rate of change $f_{carr,doppler,satellite}$ and $f_{carr,doppler,user}$ and local clock frequency error $f_{carr,clock}$ as

$$f_{carr} = f_{carr,clock} + f_{carr,doppler,user} + f_{carr,doppler,satellite} \tag{5}$$

The different frequency errors are bounded assuming a user on earth, a maximum user velocity of 50m/s and an oscillator accurate to within 2 ppm (assumption 5). This gives

$$-4\,\text{kHz} < f_{carr,doppler,satellite} < +4\,\text{kHz}$$
$$-300\,\text{Hz} < f_{carr,doppler,user} < +300\,\text{Hz}$$
$$-3.2\,\text{kHz} < f_{carr,clock} < +3.2\,\text{kHz}$$
$$-8\,\text{kHz} < f_{carr} < +8\,\text{kHz}$$

[1] The complexity of the FFT algorithm is $O(NlogN)$, even for large prime N, but FFT implementations are generally better optimized for lengths that are a power of two.

The bounds on f_{carr} will be used consistently throughout this paper.

3 SERIAL SEARCH

The purpose of acquisition is to detect a signal that may be present, and also estimate the code phase (τ) and carrier frequency (f_{carr}). As the signal power at the antenna (around -130 dBm in open sky conditions) is significantly below the noise floor (typically -111 dBm for a 2 MHz bandwidth(Akos et al., 2000)), the signal is summed over an integration time T_c to increase the SNR. This is coupled with mixing to baseband (as the carrier frequency is unknown) and correlation with a replica of the pseudonoise vector PN_{sv}. The serial search algorithm consists of evaluating

$$c\left[\hat{n},\hat{f}_{carr}\right] = \left| \sum_{n=\hat{n}}^{\hat{n}+T_c f_{s_0}} s[n] e^{-i2\pi \frac{\hat{f}_{carr}}{f_{s_0}} n} PN_{sv}\left(\frac{f_{code_0} n}{f_{s_0}}\right) \right| \quad (6)$$

where c is the correlation result, s is the data from the front-end, the exponential term mixes the signal to baseband, and PN_{sv} is the pseudonoise vector. $\hat{n}$ is the codephase expressed as samples and $\hat{f}_{carr}$ is the candidate carrier frequency. Similar to the nominal sampling frequency f_{s_0}, f_{code_0} is the nominal code frequency 1.023 MHz. The correlation result c is thus a two dimensional array evaluated over $N_n N_f$ values where N_n is the number of code phases and N_f is the number of frequencies. It should be stressed that this algorithm is very inefficient and not recommended for software implementations, rather it is used as an example around which key points are discussed. In the next section, an improved algorithm is presented.

Let us consider a T_c of 1 ms (typically sufficient for open sky scenarios) and $N_n = 2048$ (every sample) and $N_f = 25$ ($\Delta f_{carr} = \frac{2}{3T_c}$). Now, we can compute the probability of detecting a signal with a certain signal power and finally relate this to the computational complexity of the serial search algorithm. Following "Understanding GPS" (Kaplan and Hegarty, 2006) and assuming that the standard deviation σ_s of the noise ω is 1, the post-correlation probability distribution is

$$p\left(x|C/N_0\, T_c\right) = \begin{cases} x e^{-\left(\frac{x^2}{2} + C/N_0 T_c\right)} I_0\left(x\sqrt{2C/N_0 T_c}\right), & x \geq 0 \\ 0, & x < 0 \end{cases} \quad (7)$$

where x is the amplitude and C/N_0 (carrier to noise ratio) is a bandwidth independent expression of SNR. I_0 is the modified bessel function of the first kind and zero order. When $C/N_0 = 0$ (no signal present), equation 7 reduces to the Rayleigh distribution.

Figure 1 shows an illustration of the noise and signal+noise distributions. A threshold V_t is chosen such that the probability of false alarm (P_{fa}, the integral of $p(x|0)$ from V_t to ∞) is sufficiently small. For a given C/N_0 (in this case 38 dBHz), the integral of $p(x|C/N_0)$ from 0 to V_t represent the likelihood of a missed detection P_{md}. It should be noted that P_{fa} only denotes the single trial probability. When the search space $N_n N_f$ grows, so does the risk that the algorithm will erroneously detect a false peak. The likelihood of a false peak $P_{fa|\breve{M}}$ given $\breve{M}$ independent and identically distributed trials is

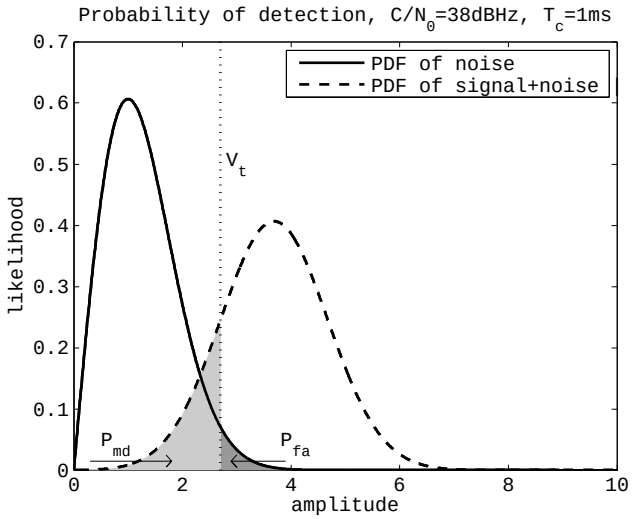

Figure 1. Illustration of P_{fa} and P_{md}

$$P_{fa|\breve{M}} = 1 - (1 - P_{fa})^{\breve{M}} \quad (8)$$

There are also two additional effects that are not considered thus far. Equation 7 assumes that the pseudonoise replica will match up perfectly with the signal $s[n]$. However, the replica may be slightly offset both in codephase and in frequency. The correlation peak is a triangle as a function of codephase offset, and a sinc as a function of doppler offset. For the values given in the example, a correlator spacing of 1 sample ≈ 0.5 chip, the acquisition process are only guaranteed 75% of the signal power. With the quoted doppler spacing of $\Delta f_{carr} = \frac{2}{3T_c}$, the worst case is that the remaining signal power is reduced to $\text{sinc}\left(\frac{1}{3}\right) \approx$ 83% of that. This means that equation 7 is not fully applicable to the process, and also that the different trials are not fully independent ($\breve{M}$ is smaller than the number of actual trials M).

The assumption

$$\frac{M}{4} \leq \breve{M} \leq \frac{M}{2} \Rightarrow \breve{M} \approx \frac{3M}{8} \quad (9)$$

is believed to be a reasonable approximation and not investigated further. The issues regarding the code phase and frequency spacing can be solved by considering them as additional stochastic variables and computing an accurate (however discrete approximation) of the probability distri-

bution function. It will be

$$\breve{p}(x|\mathbf{K}) = \begin{cases} \frac{1}{N_K}\sum_{i=0}^{N_K-1} e^{-\left(\frac{x^2}{2}+\mathbf{K}[i]\right)} I_0\left(x\sqrt{2\mathbf{K}[i]}\right), & x \geq 0 \\ 0, & x < 0 \end{cases} \tag{10}$$

where $\mathbf{K}$ is a vector (with N_K elements) composed of

$$\mathbf{K} = \left(\mathbf{K}_{\Delta\tau} \otimes \mathbf{K}_{\Delta f}\right) C/N_0 T_c \tag{11}$$

The symbol $\otimes$ denotes the kronecker tensor product of the two vectors

$$\mathbf{K}_{\Delta\tau} = \frac{3 f_{code_0}}{2 f_{s_0}} \ldots 1 \tag{12}$$

$$\mathbf{K}_{\Delta f_{carr}} = \operatorname{sinc}\left(0 \ldots \Delta f_{carr} \frac{T_c}{2}\right) \tag{13}$$

with $\sqrt{K_N}$ elements each. The "..." notation means linearly distributed between the two edge cases. This technique will be expanded later to resolve additional issues.

Returning to the determination of $P_{fa|\breve{M}}$ and P_{md}. If we set $P_{fa|\breve{M}} = 0.01$ (meaning that our acquisition process will report a false peak 1% of the time), and $P_{md} = 0.5$, the minimum C/N_0 that is detectable half the time can be found. As equation 10 is not a closed form expression, we resort to numerical methods. The PDF is evaluated over a fine grid, $\mathbf{K}$ is taken into account according to the stated formula, and the value of C/N_0 that gives the the correct V_t is searched for using iterative methods. This means that an alternative approach to equation 11, the convolution between the analytic expressions of the PDF of the variables in equation 12 and 13, is worthwhile. In order to reduce the computational expense of the simulation, K may need to be sorted and downsampled to a reasonable size.

For our example, this gives

$$\begin{aligned} M &= N_n N_f = 51200 \\ \breve{M} &= \frac{3M}{8} = 19200 \\ P_{md|\breve{M}} &= 1 - (1 - P_{md})^{\frac{1}{\breve{M}}} \approx 5 \cdot 10^{-7} \\ V_t &= \sqrt{-2\log\left(P_{md|\breve{M}}\right)} \approx 5.38 \\ C/N_0 &\approx 42.3\text{dBHz} \end{aligned} \tag{14, 15}$$

The value of C/N_0 derived like this is referred to as the minimum detectable C/N_0 (as it is the lowest powered signal that fulfills a P_{md} of 0.5), although lower power signals may obviously also be detected.

A translation of equation 6 to pseudocode is shown in table 1. A closer inspection of the program reveals that the innermost loop (line 6 through 9) will require the number and type of operations (please note that operations on complex numbers are suffixed with a c) as shown in table 2.

line	additions	multiplications	comparisons	indexing
6	1	0	1	0
7	2	0	0	0
8	1c	5c	0	3
9	0	0	0	0

Table 2. Number of operations of the innermost loop of the serial search algorithm

These lines constitutes the absolute majority of the computational expense, so the other lines in the algorithms can be ignored. For a given hardware platform, the algorithm can be implemented and evaluated with regards to the parameter of interest (for example processing time or power consumption). However, in order to provide a metric of the total computational expense for a general computing platform, the following assumptions have been made. Integer and floating point additions/multiplications both use 1 operation (op). Real addition and multiplication require 1 op. Complex addition use 2 ops and complex multiplication use 6 ops. A comparison need 1 op. Regarding the indexing, $s[n]$ is assumed to require 1 op. The *mod* function is used in both *exp* and *PN*, and it is implemented as

$$a \mod b = a - b\,\text{floor}\left(\frac{a}{b}\right) \tag{16}$$

Thus the *mod* function requires 4 ops. For the *PN* function, this is followed by 1 additional op (the indexing). The *exp* function is split into *sin* and *cos* parts and requires an additional 3 ops (indexing, addition plus indexing). The total number of ops for the innermost loop is then (summarized by column) $4+30+1+(1+7+5) = 48$. This loop will, for the worst case where the peak is not found, be executed $N_f N_n^2$ times, for our example requiring around 5 Gops.

The method proposed above can be used to evaluate any acquisition algorithm, and different settings of the parameters can be tested (in this case T_c and Δf_{carr}). For a Δf_{carr} of 1 kHz instead of $\frac{2}{3}$ kHz, the minimum detectable C/N_0 is only marginally larger (42.5 dBHz instead of 42.3 dBHz) while requiring only 3.4 Gops. If T_c is increased to 2 ms, an additional effect comes into play. In the worst case, a data bit switch will occur at the start of the 2nd code period, reducing the signal energy of the integration period to 0. Similar to how the code phase offset and carrier offset was treated, the data bit switch can be treated as a stochastic variable. The data bits are 20 code periods, and the sign could be either the same or different as the previous data bit. It has a likelihood of $\frac{1}{40}$ of being 0 and 1 elsewhere. This can be accounted for by extending equation 11 with an additional vector representing this loss.

For $T_c = 2$ ms and $\Delta f_{carr} = \frac{2}{3T_c}$, this gives a minimum

line	code	comment
1	$x = f_{code_0}/f_{s_0}$	Compute chips/samples ratio
2	for $i_1 = 1 \ldots N_f$	Code phase offset
3	$y = -i2\pi/f_{s_0}(i_1 - (N_f+1)/2)\Delta f_{carr}$	Frequency step between samples
4	for $i_2 = 1 \ldots Nn$	Frequency offset
5	$z = 0$	Set correlation sum to 0
6	for $i_3 = 1 \ldots Nn$	Summation loop
7	$n = i_2 + i_3 - 1$	index
8	$z = z + s[n]\exp(yn)PN(xn)$	Correlation sum
9	end	
10	if abs$(z) > V_t$	Check for peak
11	break	Exit program
12	end	
13	end	
14	end	

Table 1. Pseudo code of the serial search algorithm

detectable C/N_0 of 39.8 dBHz. The corresponding operation count is 39 Gops.

4 COHERENT FFT ACQUISITION

The serial search algorithm presented in the previous section have been used in real receivers (however more advanced detectors are usually implemented). Following the paper of vanNee (van Nee and Coenen, 1991) and the advent of software receivers, FFT based acquisition algorithms became a viable option. The principle is fairly straight forward. Similar to how convolution in the time domain equal multiplication in the frequency domain, correlation in the time domain equal multiplication in the frequency domain with a complex conjugate on one of the vectors. This section focus on the performance and complexity of a coherent FFT based acquisition algorithm.

Similar to equation 6, the FFT acquisition algorithm is

$$\mathbf{c}_{f_{carr}} = \text{IFFT}\left(\text{FFT}\left(\mathbf{b}_{\hat{f}_{carr}}\right) \odot \overline{\text{FFT}\left(\mathbf{pn}\right)}\right) \qquad (17)$$

where $\odot$ denotes elementwise multiplication and the overline complex conjugate. The vectors $\mathbf{b}_{\hat{f}_{carr}}$ and $\mathbf{pn}$ is defined as

$$\begin{aligned} b_{\hat{f}_{carr}}[n] &= s[n]\mathrm{e}^{\left(-j2\pi\frac{\hat{f}_{carr}}{f_{s_0}}n\right)} \\ pn[n] &= PN_{sv}\left(\frac{f_{code_0}}{f_{s_0}}n\right) \end{aligned} \qquad n = 0 \ldots f_{s_0}T_c - 1 \quad (18)$$

Table 3 shows equation 17 translated to pseudo code. Regarding the computational complexity of the FFT algorithm, several papers have been published. Of particular interest here is the flop (floating point operations) count where recent results (Lundy and van Buskirk, 2007), and also (Johnson and Frigo, 2007), suggest for example that a 2048 elements complex FFT can be computed using 75688 flops. As an approximation, 1 flop will be assumed to equal 1 op. Also, it will be assumed that the IFFT can be computed with the same number of ops (only slightly optimistic). The total op count of the algorithm for each line is also shown in the table. The total sum is

$$N_{ops} = N_{fft} + N_f\left(16 + 10N_n + 2N_{fft}\right) \qquad (19)$$

such that when $f_{s_0} = 2.048\,\text{MHz}, T_c = 1\,\text{ms}, \Delta f_{carr} = \frac{2}{3T_c}(N_f = 25, N_n = 2048, N_{fft} = 75668)$ evaluates to around 4.4 Mops, a significant reduction over the serial search implementation.

The detection performance of the FFT-based acquisition routine is however not as good as the serial search implementation. This is due to that a data bit shift could occur anywhere in the data vector $s[n]$. With the serial search, twice as much data as the integration period is used, while the latter algorithm computes a circular correlation using only one integration period of data. This effect can be modeled similar to how the likelihood of a data bit switch for the 2 ms integration period was taken into account. It is a 1 in 40 risk that a data bit switch occurs in 1 ms of data, and should this occur the signal power factor is linearly distributed between 0 and 1. For our example $T_c = 1\,\text{ms}(N_n = 2048)$ and $N_f = 25$, this effect is marginal and the minimum detectable C/N_0 is 42.3 dBHz. For longer integration periods, the effect is more noticeable.

5 NON-COHERENT FFT ACQUISITION

In this section, an extension of the FFT based coherent acquisition algorithm is presented to allow for non-coherent summations. This is expressed as

$$\mathbf{c}_{N_s,\hat{f}_{carr}} = \sum_{n=0}^{N_s-1}\left|\text{IFFT}\left(\text{FFT}\left(\mathbf{b}_{n,\hat{f}_{carr}}\right) \odot \overline{\text{FFT}\left(\mathbf{pn}\right)}\right)\right|^2 \qquad (20)$$

where N_s is the number of non-coherent summations and n is the data block index. The squaring and summing was

line	code	ops	comment
1	$\mathbf{v}_1 = conj(FFT(\mathbf{pn}))$	N_{fft}	Complex conjugate of the FFT of the code
2	for $i_1 = 1 \ldots N_f$	$2N_f$	Frequency offset
3	$x = -i2\pi/f_{s_0}(i_1 - (N_f+1)/2)\Delta f_{carr}$	$8N_f$	Frequency step between samples
4	$\mathbf{v}_2 = \exp(y \cdot [0 \ldots N_n - 1])$	$8N_fN_n$	generate $\mathbf{b}_{\hat{f}_{carr}}$
5	$\mathbf{v}_3 = FFT(\mathbf{v_2})$	N_fN_{fft}	Compute FFT of data
6	$\mathbf{v}_4 = \mathbf{v}_3 \odot \mathbf{v}_1$	$6N_f$	Element wise multiplication
7	$\mathbf{v}_5 = IFFT(\mathbf{v}_4)$	N_fN_{fft}	IFFT of the result
8	for $i_3 = 0 \ldots N_n - 1$	N_fN_n	Loop over n
9	if $v_5[i_3] > V_t$	N_fN_n	
10	break		exit program
11	end		
12	end		
13	end		

Table 3. Pseudo code of the coherent FFT based acquisition algorithm

first proposed by Marcum (Marcum, 1960) (where it is referred to as the square law detector). This algorithm ignores the phase information and as a consequence, the search space $\breve{M}$ remains constant.

Starting from equation 7, the probability distribution function of the noise when implementing equation 20 can be found. The squaring is represented by the function $g(x) = x^2$ and this means that

$$p\left(x^2|0\right) = \frac{p(x|0)}{g'(x)} = \frac{1}{2}e^{-\frac{1}{2}x} \tag{21}$$

and the summation of 2 random variables belonging to this distribution can be found by the convolution integral. For $N_s \in [2,4,8,16]$, the corresponding distribution functions are

$$p_2(x^2|0) = \frac{x}{4}e^{\left(-\frac{x}{2}\right)} \tag{22}$$

$$p_4(x^2|0) = \frac{x^3}{96}e^{\left(-\frac{x}{2}\right)} \tag{23}$$

$$p_8(x^2|0) = \frac{x^7}{1290240}e^{\left(-\frac{x}{2}\right)} \tag{24}$$

$$p_{16}(x^2|0) = \frac{x^{15}}{85699747381248000}e^{\left(-\frac{x}{2}\right)} \tag{25}$$

$$\tag{26}$$

where the subscript immediately following p denotes the number of non-coherent summations. This PDF can be integrated to find the threshold V_t. For the case of noise+signal, it is slightly more complicated. As equation 10 should be used, a discrete approximation is required. Start by evaluating p_{N_s} as a function of $\sqrt{x}$ over a fine grid. Divide the result by $\sqrt{x}$. p_{N_s} is now a discrete approximation as a function of x. The summation of several random variables can then be found by convolving the two vectors using the approach suggested by Requicha (Requicha, 1970). With this method the minimum detectable C/N_0 can be found for given values of N_n, N_f, N_s.

Table 5 shows an implementation in pseudo code of equation 20. The total op count is

$$N_{op} = N_{fft} + N_n + N_f\left(11 + 13N_n + N_s\left(11 + 11N_n + 2N_{fft}\right)\right) \tag{27}$$

While neither of the algorithms presented here can be said to be optimal, the latter two lend themselves well to analysis while being reasonably fast. The minimum detectable C/N_0 and required op count for the non-coherent algorithm have been computed for the following values of $T_c, \Delta\hat{f}_{carr}$ and N_s,

$$T_c \in [1,2,4,\ \ldots\ ,16]\,\text{ms} \tag{28}$$

$$\Delta\hat{f}_{carr} \in \left[\frac{2}{3T_c}, \frac{3}{3T_c}, \frac{4}{3T_c}\right] \tag{29}$$

$$N_s \in \left[1,2,4,\ \ldots\ \frac{16}{1000T_c}\right] \tag{30}$$

When $N_s = 1$, the op count of the coherent FFT based acquisition routine 19 have been used instead.

Figure 2 shows the operation count as a function of minimum detectable C/N_0. Values from the same set of T_c and N_c have been connected with a line, while values with the same $\Delta\hat{f}_{carr}$ share a common symbol. The number of non-coherent summations start at 1 (meaning a pure coherent algorithm) to the right and increase by a power of 2 for each sample along the line to the left.

6 CONCLUSION

In this paper a novel method for computing the probability of false alarm/missed detection for acquisition of GPS signals have been presented. It is based on accurate discrete approximations of the probability density functions. While the discrete approximations have clear disadvantages (iterative methods are required to solve for key parameters), it does allow for taking additional parameters into account.

line	code	ops	comment
1	$\mathbf{v}_0 = conj(FFT(\mathbf{pn}))$	$N_{fft}+N_n$	Complex conjugate of the FFT of the code
2	for $i_1 = 1 \ldots N_f$	$2N_f$	Loop over frequency offset
3	$\mathbf{v}_1 = 0$	$N_f N_n$	set result vector to zero
4	$x = -i2\pi/f_{s_0}(i_1 - (N_f+1)/2)\Delta f_{carr}$	$N_f 8$	Frequency step between samples
5	$\mathbf{v}_2 = exp(x \cdot [0 \ldots N_n - 1])$	$N_f 8 N_n$	Generate freq. vector
6	for $i_2 = 0 \ldots N_s$	$N_f 2 N_s$	Loop over data blocks
7	$\mathbf{v}_3 = s[N_s N_n + [0 \ldots N_n - 1]] \odot \mathbf{v}_2$	$N_f N_s(1+7N_n)$	data mixed to baseband
8	$\mathbf{v}_4 = FFT(\mathbf{v}_3)$	$N_f N_s N_{fft}$	Convert to freq. domain
9	$\mathbf{v}_5 = \mathbf{v}_4 \odot \mathbf{v}_0$	$N_f N_s 6$	Multiplication in freq. domain
10	$\mathbf{v}_6 = IFFT(\mathbf{v}_5)$	$N_f N_s N_{fft}$	convert to time domain
11	$\mathbf{v}_7 = real(\mathrm{v}_6)$	$N_f N_s$	Real part of correlation
12	$\mathbf{v}_8 = imag(\mathrm{v}_7)$	$N_f N_s$	Imaginary part of correlation
13	$\mathbf{v}_1 = \mathbf{v}_1 + \mathbf{v}_7 \odot \mathbf{v}_7 + \mathbf{v}_8 \odot \mathbf{v}_8$	$N_f N_s(4N_n)$	Add to result
14	end	-	
15	for $i_3 = 0 \ldots N_n$	$N_f 2 N_n$	Loop over samples
16	if $v_1[i_3] > V_t$	$N_f N_n 2$	Check for peak
17	break	-	exit program
18	end	-	
19	end	-	
20	end	-	

Table 4. Pseudo code of the non-coherent FFT based acquisition algorithm

As an example, the impact of correlator and doppler spacing, as well as the likelihood of data bit switches, have been considered. All three parameters have here been modeled as stochastic variables, and this may or may not be a valid assumption. For example, a receiver with a good estimate of time and a recent almanac, can predict the possible data bit switches. The data shown here are thus only valid for blind acquisition where the receiver have no such a priori information, although the methods presented are general and can be modified for other applications.

The second contribution of the paper consist of an analysis of the computational complexity of different acquisition algorithms. Focus is on software based receiver architectures, and sophisticated detectors such as the Tong or M of N detector (Kaplan and Hegarty, 2006) is not considered.

It is shown that the FFT-based algorithms clearly outperforms the time domain correlation implementation with regards to the number of operations (this is not surprising). To facilitate the analysis, a general computing platform have been assumed. Depending on the intended hardware platform for an actual implementation, the results may be different. Unfortunately, modern pipelined processor architectures are difficult to analyze and we are thus forced to consider a more general computing engine.

Nevertheless, the simulations suggest that non-coherent summations with a short coherent integration interval should be preferred over longer coherent integration intervals, at least in the evaluated region of 33 dBHz to 42 dBHz given the additional assumptions discussed in previous sections.

REFERENCES

Akos, D. (1997). *A Software Radio Approach to Global Navigation Satellite System Receiver Design*. PhD thesis, Ohio University.

Akos, D., Normark, P.-L., Lee, J.-T., Gromov, K., Tsui, J., and Schamus, J. (2000). Low power global navigation satellite system (GNSS) signal detection and processing. *Proc. ION GPS*.

Bastide, F., Akos, D., Macabiau, C., and Roturier, B. (2003). Automatic gain control (AGC) as an interference assessment tool. *Proc. ION GNSS*.

Beaulieu, N. (1990). An infinite series for the computation of the complementary probability distribution function of a sum of independent random variables and its application to the sum of rayleigh random variables. *IEEE tran. comm.*, 38(9):1463–1474.

Johnson, S. and Frigo, M. (2007). A modified split-radix FFT with fewer arithmetic operations. *IEEE Tran. signal processing*, 55(1):111–119.

Kaplan, E. and Hegarty, C. (2006). *Understanding GPS, Principles and Applications*. Artech House.

Lowe, S. (1999). Voltage signal-to-noise ratio (SNR) nonlinearity resulting from incoherent summations. *TMO Progress Report*, 42-137.

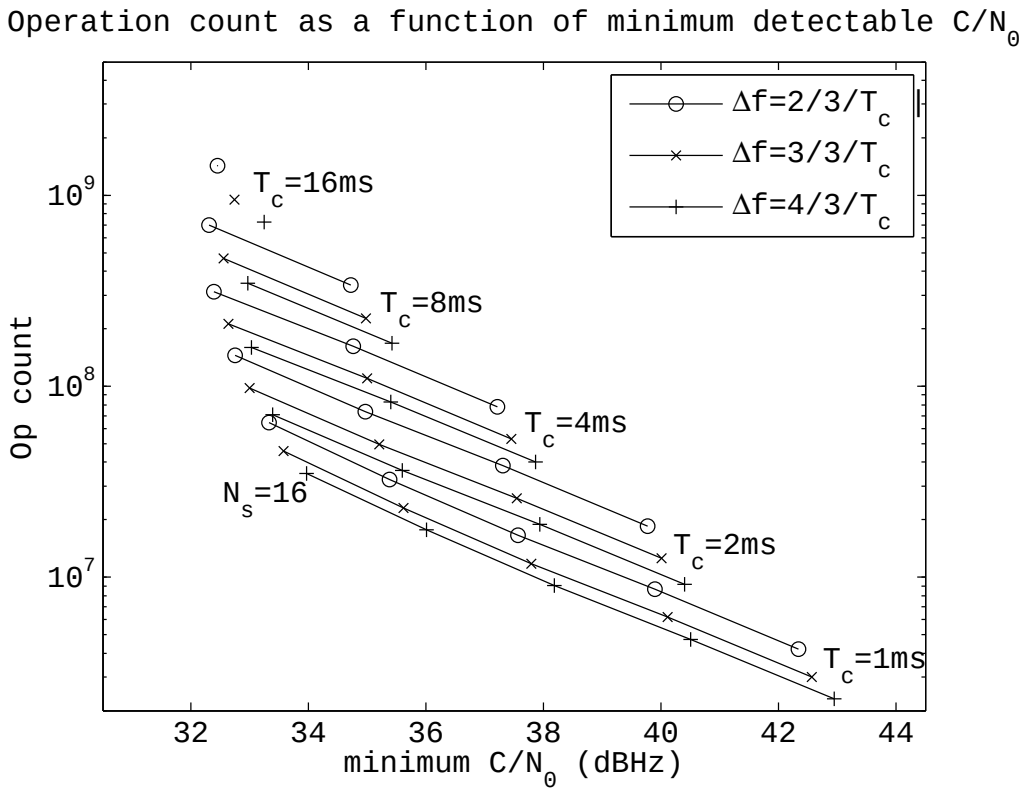

Figure 2. Minimum detectable C/N_0 and operation count

Lundy, T. and van Buskirk, J. (2007). A new matrix approach to real FFTs and convolutions of length 2^k. *Computing*, 80(1):23–45.

Marcum, J. I. (1960). A statistical theory of target detection by pulsed radar. *IRE Tran. on Information Theory*, 6:59–267.

Psiaki, M. (2001). Block acquisition of weak GPS signals in a software receiver. *Proc. ION GNSS*.

Requicha, A. (1970). Direct computation of distribution functions from characteristic functions using the fast fourier transform. *Proc. of the IEEE*, 58(7):1154–1155.

van Dierendonck, A., Fenton, P., and Ford, T. (1992). Theory and performance of narrow correlator spacing in a GPS receiver. *Journal of the ION*, 39(3):265–283.

van Nee, D. and Coenen, A. (1991). New fast GPS code-acquisition techniquee using FFT. *Electronics Letters*, 27(2):158–160.